Small-Angle X-ray Scattering from Dilute Solutions of Substituted Phthalocyaninato–Polysiloxanes

Thomas Sauer† and Gerhard Wegner*

Max-Planck-Institut für Polymerforschung, Ackermannweg 10, Postfach 3148, D-6500 Mainz, FRG

Received August 6, 1990

ABSTRACT: The dilute-solution properties of alkoxy-substituted phthalocyaninato–polysiloxanes are investigated by using small-angle X-ray scattering (SAXS). The scattering of rodlike particles is studied with special emphasis on molecular parameters important in real polymeric systems such as polydispersity, overall length, finite cross-section, and chain flexibility. Polydispersity and finite flexibility show a strong interdependence with opposite influence on the particle scattering factor. It is shown that especially in the limit of high persistence lengths (rod limit) polydispersity plays a crucial role in determining molecular dimensions by scattering techniques. The exact form factor for a polydisperse, circular cylinder is compared to the approximate form factor for infinitely thin rods corrected for a finite cross-section. Good agreement is found in the angular range from $h = 0.05$ to 0.1 Å^{-1}. The Zimm analysis of the experimental data obtained from dilute solutions in heptane and toluene gives weight-average degrees of polycondensation typically between 50 and 160. While the fit of the radius of gyration as a function of the contour length only allows for the estimation of a lower limit of 1000 Å for the persistence length, the angular dependence of the scattered intensity agrees well with particle scattering functions of polydisperse, thick rods. Radii of gyration of the cross-section are determined to range typically between 10 and 25 Å while the polydispersity is in good agreement with a most probable distribution ($M_w/M_n - 1 = 1$). The experimental mass per unit contour length is well within the range of the theoretical values, indicating the absence of aggregation in the concentration regime investigated. Besides the conventional Zimm extrapolation, which is nonlinear for rodlike particles, several linear methods arising from the asymptotic scattering behavior of rodlike particles are discussed and applied to the experimental data after elimination of the cross-section factor. Data from both treatments show a good agreement and moreover confirm the rodlike chain conformation of the polymers.

Introduction

Phthalocyaninato–polysiloxane (PCPS) has been studied for several years because of its unusual molecular structure, which gives rise to conductivity phenomena in the solid state when reacted with oxidants.[1] The close cofacial packing of the monomer units along the polysiloxane chain, which is shown in Figure 1, leads to a rather strong interaction between repeat units, which results in a Si–O–Si bond angle of nearly 180°. This unusual geometry has been verified from the crystal structure of oligomeric model compounds.[2,3] Furthermore, the repeat distance of 3.33 Å is considerably smaller than the van der Waals distance between planar aromatic hydrocarbons in molecular crystals, which is usually in the range of 3.4–3.6 Å. Due to this strong steric interaction, a bending of the polymer main chain seems to be quite unprobable and indeed has not been observed experimentally so far. An ideal rodlike main-chain conformation is therefore assumed for this material, but, due to the insolubility of the parent polymer in nonreactive solvents, investigations are limited to the solid state and yet no information on the single-molecule properties is available. Especially the rodlike conformation of the macromolecules projected from solid-state structural investigations and assumed from its molecular architecture has never been proven experimentally. The solubility problem, which is the major hindrance in studying single-chain properties, can be circumvented by synthesizing the polymers from appropriately substituted phthalocyanine monomers, which has been attempted repeatedly in recent years.[4–8] So far only low molecular weight oligomers were obtained. In previous publications[9–11] we reported on novel synthetic procedures

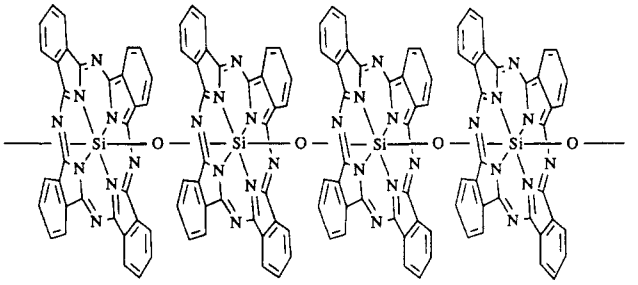

Figure 1. Sketch of the molecular structure of unsubstituted phthalocyaninato–polysiloxane (PCPS).

in order to synthesize a new class of soluble phthalocyaninato–polysiloxanes bearing flexible alkoxy side chains. The molecular structure of the monomers and polymers and particularly the chemical nature of the side chains can be seen from the reaction scheme in Figure 2. The exact knowledge of the molecular weight of these polymers is of rather basic interest since first it allows us to optimize synthetic procedures and second it is of inherent importance for the interpretation of such physical properties as liquid-crystalline phase behavior.

Scattering of electromagnetic radiation from dilute polymer solutions is the favorite experimental technique to study conformations and access molecular dimensions at the same time. Light scattering,[12] which is the most frequently used technique, cannot be applied for studying substituted PCPS since the strong interaction between the phthalocyanine chromophores leads to an enormous broadening of the optical spectrum.[13] No region of vanishing absorbance can be identified in the visible range. Two complementary methods are small-angle X-ray (SAXS) and neutron (SANS) scattering.[14,15] The SAXS technique has been successfully used for many years for studying single-molecule properties, especially the overall

† Present address: IBM Research Division, Almaden Research Center, 650 Harry Road, San Jose, CA 95120-6099.

0024-9297/91/2224-2240$02.50/0

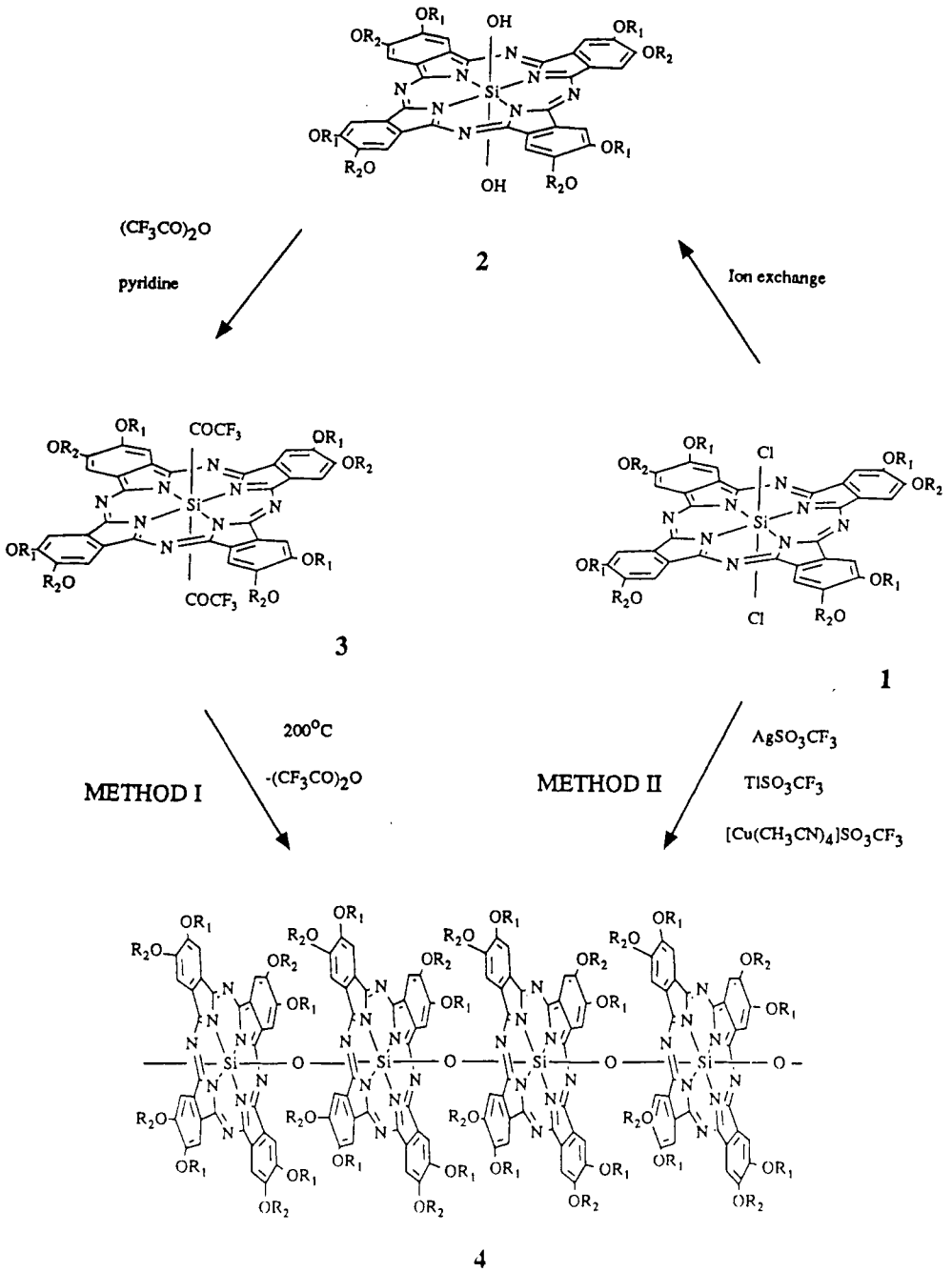

Figure 2. Synthesis of alkoxy-substituted phthalocyaninato–polysiloxanes (4) from the corresponding phthalocyaninato–dichlorosilane (1). Polymers are abbreviated throughout the text as C*n*PCPS, $R_1 = R_2 = C_nH_{2n+1}$ where n = 2, 4, 6, ..., 18, and C1C8PCPS, $R_1 = CH_3$ and $R_2 = C_8H_{17}$.

shape and dimension of biopolymers in dilute solution.[16,17] Kirste and Wunderlich applied this technique to dilute solutions of synthetic polymers, e.g., poly(methyl methacrylates), of different tacticity, in a range of molecular weights too small for light scattering. Their results demonstrate the sensitivity of the method for local chain conformations[18-20] since they could resolve the different chain conformations that arise from different stereochemical microstructures. Instrumental improvements[14] and the availability of SANS[21,22] have widened this field of research enormously. Using these techniques as experimental tools, the chain conformation of polyelectrolytes[23] and conjugated polymers,[24,25] among others, is of very recent interest.

Some preliminary results from SAXS investigations in dilute solution[10] indicate that the alkoxy-substituted PCPS have a rather high molecular weight and that the chain conformation is best described as a rigid rod of considerable thickness. In this paper we want to discuss the single-chain properties of these polymers in more detail based on SAXS measurements on a number of different samples. In the first part, the basic relations from scattering theory of rigid rods are discussed with special emphasis on polydisperse materials. Furthermore, the influence of a variety of parameters that play a role in real polymeric systems is analyzed numerically, and the way the appearance of the scattering curves is affected by them is discussed. In the second part, experimental results from SAXS measurements from substituted phthalocyaninato–polysiloxanes in dilute solution will be presented and analyzed using the theoretical background discussed before. Finally the data will be critically compared, and the results for the molecular conformation will be discussed for their meaning for further physical properties of these polymers.

Experimental Section

Substituted phthalocyaninato–polysiloxanes were obtained from the corresponding phthalocyaninato–dichlorosilanes (1) or –dihydroxysilanes (2) by condensation methods reported elsewhere.[10,11] Figure 2 gives a schematic overview of the chemistry involved, particularly the active ester route (method I) and the polycondensation using halogenophilic trifluoromethanesulfonates as condensation reagents (method II). The molecular structure of the resulting polymers is in agreement with results from spectroscopic characterization.

Small-Angle X-ray Scattering. A conventional Kratky compact camera with a block collimation system (Anton Paar KG) was used together with a position-sensitive detector (MBraun) having a spatial resolution of approximately 80 μm. In order to control the sample temperature, a commercial sample flow cell was equipped with a vacuum-resistant water circuit connected to an external thermostat. The sample temperature could be varied between 10 and 80 °C with a relative accuracy of ±0.03 °C. The absoloute intensity was measured by a moving slit device.[26] Ni-filtered Cu Kα radiation was used together with a pulse-height discriminator. All measurements were done with an entrance slit width of 80 μm. Polymers were dissolved in analytical-grade solvents with concentrations varying between 2 and 10 mg/mL. The density of dilute polymer solutions was measured with a DMA 60 device (Anton Paar KG).

Data Acquisition and Treatment. The experimental conditions for measuring scattering curves were chosen in such a way as to achieve a statistical error smaller than 1% at all measured angles. Usually measuring times between 5 and 10 h were required for each concentration. These data were corrected for absorption as determined by the moving slit device, and the normalized scattering curve of the pure solvent was subtracted in order to obtain the scattering curve of the polymer. Smearing effects according to slit length, slit width, and wavelength distribution of the incoming radiation were eliminated by using the method of Glatter.[27-28] The desmeared intensity $I(h)$, where $h = 4\pi/\lambda \sin(\theta/2)$ denotes the magnitude of the scattering vector (λ = 1.5418 Å, θ = scattering angle), was plotted for a whole concentration series according to Zimm[29]

$$\frac{Kc}{I(h)} = \frac{1}{M_w}\left(1 + \frac{\langle R^2\rangle_z}{3}h^2\right) + 2A_2c \tag{1}$$

to give the weight-average molecular weight M_w, the z-average mean-square radius of gyration $\langle R^2\rangle_z$, and the second virial coefficient of the osmotic pressure A_2. c denotes the mass concentration of the polymer solution, and the contrast factor K is given by[16]

$$K = \frac{P_0 \Delta z^2 r_e^2 d N_L}{a^2} \tag{2}$$

N_L is Avogadro's number, d the thickness of the sample cell (0.1 cm), r_e the scattering radius of an electron ($r_e^2 = 7.93 \times 10^{-26}$ cm^2), P_0 the integral primary beam intensity, and a the distance between sample and detector (23.5 cm). The electron density difference Δz between solute and solvent is given by

$$\Delta z = z_2 - \nu_2^* \rho_1 z_1 \tag{3}$$

where z_1 and z_2 are the electron densities of solvent and solute, ρ_1 is the mass density of the solvent, and ν_2^* is the partial specific volume of the polymer. ν_2^* is derived from density measurements from dilute polymer solutions according to[30,31]

$$\nu_2^* = \lim_{w_2 \to 0}\left[\frac{1}{\rho_1}\left(1 - \frac{1}{\rho}\frac{\partial \rho}{\partial w_2}\right)\right] \tag{4}$$

or

$$\nu_2^* = \lim_{w_2 \to 0}\left[\frac{1}{\rho} - \frac{1}{\rho^2}(1 - w_2)\frac{\partial \rho}{\partial w_2}\right] \tag{5}$$

w_2 denotes the mass fraction of the polymer. Both equations gave the same results for ν_2^* within a range of error smaller than 2%.

Theory

Particle Scattering Functions for Stiff-Chain Polymers. The form factor of an infinitely thin rod (a needle) can be given in an analytical form as is also the case for Gaussian chains. Neugebauer[32] derived the expression

$$P(h) = \frac{1}{x}\int_0^{2x} \frac{\sin u}{u} du - \left(\frac{\sin x}{x}\right)^2; \quad x = \frac{hL}{2} \tag{6}$$

for a rod of length L and negligible cross-section. Simple deviations of this equation are also given by other authors.[33,34] The form factor $P(h)$ is related to the scattered intensity by the normalization relation $P(h) = I(h)/I(0)$. A simple asymptotic behavior of the scattering function eq 6 is obtained in the limit of large scattering vectors h. According to Zimm,[35] the following relation holds for the reciprocal form factor

$$\frac{Kc}{I(h)} = \frac{1}{MP(h)} = \frac{2}{\pi^2 M} + \frac{1}{\pi M_L}h \quad (h \text{ large}) \tag{7}$$

The form factor $P(h)$ itself is then given by

$$\frac{I(h)}{Kc} = MP(h) = \frac{\pi}{h}M_L - \frac{2}{h^2 L}M_L \quad (h \text{ large}) \tag{8}$$

M is the molecular weight of the (monodisperse) rodlike molecule, M_L is called the mass per unit length and is a measure for the mass density along the polymer chain in units of the contour length L. This parameter is important insofar that it can be easily calculated in most cases from the molar mass of the repeat unit and the projection of the repeat distance on the contour length. Therefore, comparison of experimental and theoretical values can give evidence for aggregation phenomena, the knowledge of which is important when single-chain properties are discussed.

So far only monodisperse rods have been considered. Synthetic polymers usually show a considerable amount of polydispersity, which modifies the scattering behavior quite drastically. In the case of rods of constant cross-section, this molecular weight distribution is equivalent to a polydispersity in rod length L. The probability density $w(L)$ of such a length distribution is defined such that $w(L)\,dL$ is the probability of a single molecule of the whole ensemble having the length L. One of the most widely used distribution functions is the Schulz–Flory distribution defined by

$$w(L) = \frac{y^{z+1}}{z!}L^z \exp\{-yL\} \tag{9}$$

where

$$y = \frac{z+1}{L_w}; \quad \frac{L_w}{L_n} - 1 = \frac{1}{z}$$

The two independent parameters of this distribution function are z as a measure of the polydispersity and the weight-average rod length L_w. y follows from eq 9 by the normalization condition

$$\int_0^\infty w(L)\,dL = 1 \tag{10}$$

The application of eq 9 can be expanded from using only integer values of z (since $z!$ is only defined for z being an integer) to positive real values by using the relation

$$z! = \Gamma(z+1) \tag{11}$$

The gamma function $\Gamma(x)$ is defined for real arguments x.

Applying this polydispersity correction to the particle scattering function (eq 6), Holtzer[36] obtained the following asymptotic form of the reciprocal form factor for polydisperse rods:

$$\frac{Kc}{I(h)} = \frac{1}{M_w P(h)} = \frac{2}{\pi^2 M_n} + \frac{1}{\pi M_L} h \quad (h \text{ large}) \qquad (12)$$

Here M_n and M_w are the number- and weight-average molecular weights. Inversion of this relation leads to

$$\frac{I(h)}{Kc} = M_w P(h) = \frac{\pi}{h} M_L - \frac{2}{h^2 L_n} M_L \quad (h \text{ large}) \qquad (13)$$

Equations 12 and 13 are very important in the interpretation of the scattering data from rodlike polymers, as will be demonstrated later.

The relations discussed so far have been derived for infinitely thin rods. In the case of most real polymeric systems, and especially for the substituted phthalocyaninato–polysiloxanes, such an approximation will not be valid any longer because of the considerable cross-section of these materials. Powder X-ray diffraction measurements on the bulk polymers[37] show that the diameters of these rodlike macromolecules are ranging between 25 and 40 Å, depending on the side-chain length. A very simple approximation toward this problem is an additional cross-section factor $\phi(h)$[38,39] so that the overall form factor is given in the general form

$$P(h) = P_0(h)\, \phi(h) \qquad (14)$$

where $P_0(h)$ is the form factor of the infinitely thin rod according to eq 6. The finite cross-section of a polymer chain has been taken into account for the first time by Kirste[40] in his calculations of particle scattering functions based on the Kratky–Porod model. Flory and co-workers[41] gave a nice illustration of this effect in their calculations of the form factor of poly(isobutylene) based on the rotational isomeric state model where the cross-section has been varied by considering different atoms along the polymer chain as scattering centers. Both these theoretical papers show that a finite cross-section leads to a considerable decrease in scattered intensity at large scattering angles. The neutron scattering results reported by Rawiso et al.[42] on dilute solutions of polystyrenes, deuterated in different positions in order to influence the molecular cross-section sensitive to scattering, give a nice experimental verification of this finding.

In first approximation, the cross-section $\phi(h)$ can be analytically given as a Guinier-type factor[20] so that eq 14 takes the form

$$P(h) = P_0(h) \exp\left\{-\frac{R_c^2}{2} h^2\right\} \qquad (15)$$

R_c is the radius of gyration of the cross-section. The analytical form of the cross-section factor has been investigated in detail by Koyama.[43] He showed that the numerical factor in the exponential of eq 15 is not a constant in the general case of a particle scattering function but varies between $^1/_2$ and $^1/_3$. However, $^1/_2$ is the appropriate value in the limit of high persistence length or when axial symmetry of the distribution of scattering centers about the polymer main chain can be assumed. In analogy to the radius of gyration $\langle R^2 \rangle_z^{1/2}$ of the entire molecule, this approximation should only be valid in the range $hR_c < 1$.[44] In the present work, a consideration of a polydispersity of the cross-sectional dimension is not required since copolymers made from monomers having different diameters[11] will not be considered here. Theoretically this topic has been discussed in detail by Holtzer and Rice[45] and by Hjelm.[46]

An alternative possibility for modeling the scattering of thick, rodlike molecules is the form factor for homogeneous circular cylinders.[47] The scattering function of such a particle of length L and radius r is given by

$$P(h,L) = \int_0^{\pi/2} \left[\frac{2J_1(hr \sin\alpha)}{hr \sin\alpha} \frac{\sin\left(\frac{hL}{2}\cos\alpha\right)}{\frac{hL}{2}\cos\alpha}\right]^2 \sin\alpha \, d\alpha = \int_0^{\pi/2} \frac{\pi}{hL\cos\alpha} \left[\frac{2J_1(hr \sin\alpha)}{hr \sin\alpha} J_{1/2}\left(\frac{hL}{2}\cos\alpha\right)\right]^2 \sin\alpha \, d\alpha \qquad (16)$$

where $J_i(x)$ is the Bessel function of order i. The angle α over which the integration is carried out denotes the orientation of the cylinder axis relative to the primary beam of the scattering experiment. Polydispersity again is taken into account by averaging over the length distribution (eq 9)

$$P_z(h) = \frac{\int_0^\infty L\, w(L)\, P(h,L)\, dL}{\int_0^\infty L\, w(L)\, dL} \qquad (17)$$

Equations 16 and 17 cannot be given in analytical form but are solved numerically. The cross-sectional radius of gyration R_c is related to the radius r of the homogeneous cylinder by[38]

$$r = 2^{1/2} R_c \qquad (18)$$

A further possibility of analyzing the scattering from rigid-rod polymers arises from the application of the Kratky–Porod model of the wormlike chain[48-51] in the limit of large persistence lengths.[52] This particular chain model has been thoroughly used to determine the chain stiffness of a variety of rigid and semiflexible polymers from scattering experiments.[25,53-58] The particle scattering functions given by this model at different stages of approximation will not be discussed here but can be reviewed from the references cited.

Parameters Influencing the Scattering Functions of Stiff-Chain Polymers. The form factor of stiff-chain macromolecules is influenced by a variety of parameters such as the length of the polymer chains, their cross-section, finite chain flexibility, and polydispersity. As demonstrated in the previous section, the evaluation of all these parameters as well as their interdependence is by no means straightforward, even in the case of a rigid rod where the absence of chain flexibility gives rise to a couple of rather simple forms of the particle scattering function. Therefore, the question arises if all these parameters can be determined from experimental scattering curves and to what degree of precision. These points will be discussed in the following.

The influence and interdependence of finite flexibility and polydispersity has been studied by Schmidt et al.[59] On the basis of the form factor for wormlike chains according to Koyama,[60] these authors find that an increased chain flexibility leads to a maximum in the plot of $P(h)\,h$ as a function of h (Holtzer plot; compare eq 13) as shown in Figure 3 while the form factor of a polydisperse rod is a monotonic function with the asymptotic value

$$\lim_{h\to\infty}\left[\frac{I(h)}{Kc} h\right] = \pi M_L \qquad (19)$$

The intensity at the maximum is a function of the chain

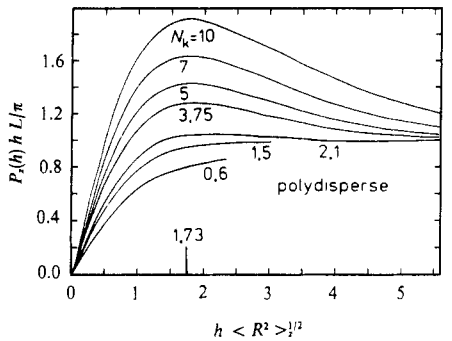

Figure 3. Normalized Holtzer plot of the particle scattering function of polydisperse, semiflexible chains as a function of the number N_k of Kuhn segments per chain (according to ref 59).

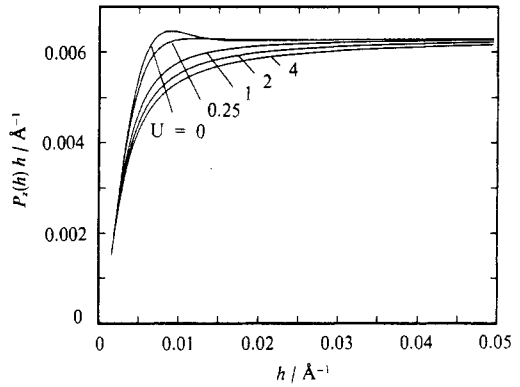

Figure 4. Holtzer plot of the particle scattering function of infinitely thin, homogeneous cylinders as a function of the polydispersity $U = M_w/M_n - 1$ (L_w = 500 Å).

flexibility, which has been successfully used to determine the persistence length of xanthan, a stiff-chain biopolymer.[61] The angular position of the maximum is shifted to higher scattering vectors with increasing polydispersity. In the case of rigid rods, the form factor also displays a maximum in the Holtzer plot when polydispersity is low (Figure 4). This structure is smeared out when the molecular weight distribution gets broader. So in both cases a similar shape of the particle scattering function is observed although the nature of their special features is essentially different. In the case of rigid rods, the local maximum is a consequence of the periodicity of the Bessel function $J_{1/2}(x)$ in eq 16. Consequently, its angular position ($hL/2 \simeq 1.5$) is a function of the rod length L_w. It has to be noted that the form factors given by eqs 6 and 16 give identical results when the cross-section of the polymer molecules is neglected. Furthermore, additional side maxima can appear when using eq 16 with a periodicity of $hr \simeq 5.4$ in the case of finite thickness represented by a nonvanishing radius r of the equivalent cylinder. From this discussion it becomes clear that it is difficult to differentiate especially between the scattering of a polymer with a persistence length q in the range $q/L_2 \lesssim 4$ and rigid rods of low polydispersity when no additional information is available.

The same difficulties appear in the interpretation of the corresponding Kratky plot where $P(h)\,h^2$ is plotted as a function of h. In this type of plot a scattering curve representing a straight line is usually interpreted as a clear sign for a rigid-rod molecular conformation while a more or less pronounced Gaussian scattering component at low scattering angles originates from finite chain flexibility. But as shown in Figure 5, a deviation from the straight line also occurs in the form factor of rigid rods having very low or no polydispersity. The reason for this behavior is

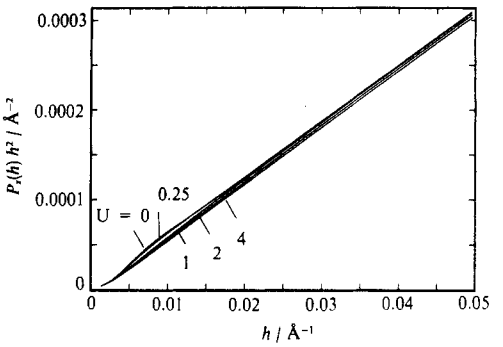

Figure 5. Kratky plot of the particle scattering function of infinitely thin, homogeneous cylinders as a function of the polydispersity $U = M_w/M_n - 1$ (L_w = 500 Å).

the same as discussed above. Obviously this feature could be misinterpreted as arising from a finite chain flexibility.

From this discussion it becomes clear that in the case of stiff polymers having a very high persistence length the finite chain flexibility and the polydispersity have an opposite influence on the scattering function. The results from analyzing scattering data, neglecting one of these factors, can cause considerable error in the other parameter. Especially the persistence length determined from fitting the scattering data has to be regarded as an upper limit when polydispersity is not rigorously taken into account.

One further point about the influence of the polydispersitty has to be discussed. The relation between molecular weight (or contour length L) and the radius of gyration has a pronounced importance for the determination of the chain stiffness since light scattering as the most convenient scattering method only covers a very small range of the scattering vector because of the large wavelength used. A reasonable fit of the experimental data to theoretical form factors is generally not possible. Benoit and Doty[62] have given the following relation for the chain dimensions of monodisperse, semiflexible polymer chains of contour length L and persistence length q

$$\langle R^2 \rangle = \frac{Lq}{3} - q^2 + \frac{2q^2}{L} - \frac{2q^4}{L^2}\left[1 - \exp\left(-\frac{L}{q}\right)\right] \quad (20)$$

Averaging over the length distribution given by eq 9, the following relation is obtained for polydisperse samples[57,63]

$$\langle R^2 \rangle_z = \frac{z+2}{z+1}\frac{L_w q}{3} - q^2 + \frac{2q^3}{L_w} - \frac{2q^4}{z(z+1)}\left[\left(\frac{z+1}{L_w}\right)^2 - \left(\frac{z+1}{L_w}\right)^{z+2}\left(\frac{z+1}{L_w} + \frac{1}{q}\right)^{-z}\right] \quad (21)$$

with the weight-average contour length L_w and the polydispersity $U = 1/z = M_w/M_n - 1$. In the limit of a rigid rod ($L_w \ll q$) this relation transforms to

$$\langle R^2 \rangle_z = \frac{(z+3)(z+2)}{12(z+1)^2} L_w^2 \quad (22)$$

In the monodisperse case all factors containing z vanish[16] so that for rigid-rod polymers the following polydispersity correction factor results:

$$\frac{\langle R^2 \rangle_{z,\text{polydisperse}}}{\langle R^2 \rangle_{\text{monodisperse}}} = \frac{(z+3)(z+2)}{(z+1)^2} \quad (23)$$

This relation clearly shows that the difference between both mean-square radii of gyration is already about 30% at a polydispersity of $U = 0.1$ ($z = 10$). Consequently, in polymers synthesized by polycondensation processes where

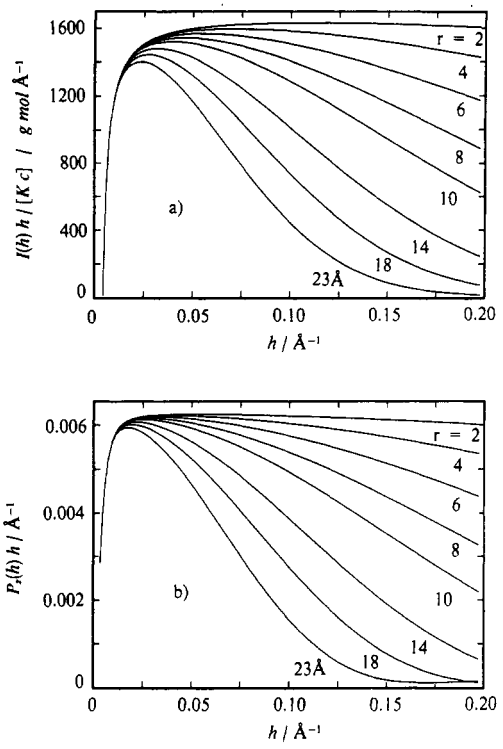

Figure 6. Holtzer plots of the particle scattering functions of rigid rods as a function of the radius r: (a) approximation according to Holtzer (eq 24); (b) exact form factor for homogeneous cylinders (eq 17). All form factors were calculated by using $U = 1$ and $L_w = 500$ Å.

the polydispersity is usually about 1 this effect cannot be neglected under any circumstances. However, eq 23 gives a possibility for determining the polydispersity of rigid rods from scattering data. Once again this relation clearly demonstrates that neglecting the polydispersity leads to a crude overestimation of the persistence length of semiflexible polymers.[57]

So far it is not known if the cross-section of rodlike molecules can be evaluated exactly using the approximation given by eq 15. By combining eqs 13 and 15, one obtains for large h values

$$\frac{I(h)}{Kc}h = M_w P(h)\, h = \left[\pi M_L - \frac{2}{hL_n}M_L\right] \exp\left\{-\frac{R_c^2}{2}h^2\right\} \quad (24)$$

This scattering function is plottted in Figure 6a for different values of R_c, which is related to the radius r of the equivalent homogeneous cylinder by eq 18. These results have to be compared to the curves obtained by the exact form factor given by eqs 16 and 17 (Figure 6b). Obviously, both methods give nearly the same results in the angular range of $0.05 \lesssim h \lesssim 0.1$ Å^{-1}. Therefore, R_c can be derived from experimental data in this region by a semilogarithmic plot of eq 24 versus h^2. Compared to the exact form factor (Figure 6b), the R_c values obtained by this procedure are systematically low, about 1 Å, which is considered to be precisely enough for practical application since the statistical error of the scattering data in this angular region is quite high because of the low scattering intensity. Furthermore, Figure 6b shows that the approximation given by eq 24 shows increasing deviations from the exact form factor for $h \lesssim 0.05$ Å^{-1} and has a singularity at $h = 0$, which is a consequence of its asymptotic nature. A better description of the low-h regime could be obtained if higher order terms are considered in the approximation given by eq 12 and subsequent relation derived therefrom.

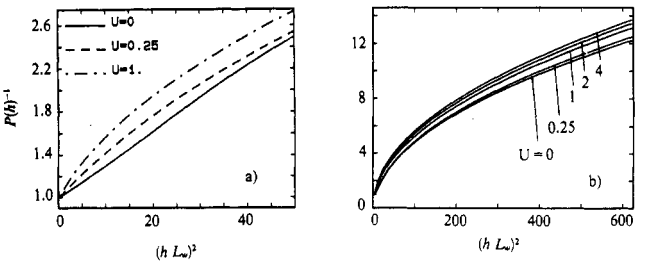

Figure 7. Zimm plot of the particle scattering function of polydisperse rigid rods: (a) infinitely thin rods (according to Goldstein[66]; (b) homogeneous cylinders in the limit of vanishing radius r (eq 17).

One final point that has to be mentioned is the influence of an inhomogeneous electron density distribution in the chain cross-section. This feature has not been considered so far. If the local deviations from the mean electron density are small, no pronounced influence on the form factor compared to the scattering from homogeneous cylinders is expected if not too high values of the scattering vector are considered ($h \lesssim 0.2$ Å). Furthermore, the interpretation of scattering data from dilute-solution measurements at $h \gtrsim 0.2$ Å^{-1} may cause substantial error since fluctuations of the solvent density about the polymer chain can have a large influence on the form factor of the cross-section in this angular region.[20,64]

Angular Dependence of the Reciprocal Particle Scattering Factor. The scattering curve at low scattering angles is of particular interest since the extrapolation according to Zimm (see eq 1) yielding the molecular weight, radius of gyration, and second virial coefficient of the osmotic pressure takes place in this angular range. A well-defined shape of the particle scattering factor within this region is required to derive these quantities unambiguously. The most preferred situation is clearly a linear functionality, which is usually obtained from scattering data of more or less flexible polymers when the reciprocal form factor is plotted as a function of h^2 (Zimm plot). However, in the case of very low polydispersity, modified procedures such as plotting $P(h)^{-1}$ as a function of h give much better linearity.[65]

The reciprocal particle scattering factor of rigid-rod molecules displays a continuous negative curvature down to very low scattering angles when plotted versus h^2. Goldstein[66] has investigated this angular dependence as a function of polydispersity. Using the form factor of an infinitely thin rod given by Neugebauer[32] (see eq 6), he showed that polydisperse rods cause a finite curvature in the Zimm plot down to $h = 0$ (see Figure 7a). Therefore, a linear extrapolation from the angular region accessible to SAXS is not possible for rigid-rod molecules, even not as a crude approximation. The Zimm plots derived from the exact particle scattering factor (eqs 16 and 17) show the same behavior (Figure 7b). It has to be noted that a finite persistence length has the same effect on the particle scattering factor as polydispersity so that also the Zimm analysis leads to an overestimation of the one parameter when the other is neglected.

A linear plot of the scattering function of rigid-rod molecules with finite cross-section in order to obtain molecular parameters such as molecular weight or radius of gyration is a priori not possible. As can be seen from Figure 6, the approximation of the particle scattering function given by eq 24 is no longer applicable in the range where the finite cross-section can still be neglected. Furthermore, the exact form factor for rigid cylinders cannot be given in an easy-to-fit, analytical form, as mentioned earlier. Therefore, it is necessary to eliminate the cross-sectional

Table I
Linear Plots for Scattering Functions of Polydisperse, Infinitely Thin Rigid-Rod Polymers

method	plot	intercept	slope
a	$I(h)\ h/Kc = f(1/h)$	πM_L	$-2M_L/L_n$
b	$I(h)\ h^2/Kc = f(h)$	$-2M_L/L_n$	πM_L
c	$Kc/I(h) = f(h)$	$2/(\pi^2 M_n)$	$1/(\pi M_L)$

dimension by evaluating R_c according to eq 15 and subsequently dividing the scattering data by the cross-section factor to obtain the form factor of the corresponding infinitely thin rod. With these data on hand, several possibilities exist to obtain linear plots making use of the asymptotic eqs 12 and 13. Table I summarizes these plots together with the analytical expressions for the slope and intercept of the linear fit. The modified Zimm plot (method c) originally proposed by Holtzer[36] is quite interesting since the intercept gives directly the number-average molecular weight. So a combination of a conventional and this modified Zimm plot gives a measure for the polydispersity $U = M_w/M_n - 1$. But, nevertheless, the determination of M_L, M_n, and L_n strongly depends on the accuracy of the determination of the cross-sectional dimension, which has to be eliminated before. It is therefore recommended to use these types of plots only within an angular region where the influence of the finite cross-section is still not very pronounced. This region can be rather narrow in the case of large cross-sections since the asymptotic nature of the basic relations gives additional limitations regarding low scattering angles.

Experimental Results

Dilute solutions of substituted phthalocyaninato–polysiloxanes show a rather high scattering contrast compared to the pure solvent, as is demonstrated by Figure 8 where the normalized, smeared scattering curves of a polymer solution and the pure solvent are compared. Suitable solvents for SAXS measurements are aliphatic and aromatic hydrocarbons since most polymer samples show a high solubility in these even at room temperature. Solubility problems in these types of solvents were only observed when very short side chains were used in combination with high molecular weights of the corresponding polymer samples. Furthermore, the absorption of the primary beam intensity, which is in the range of 50% for a sample thickness of 1 mm, is still much lower than in any solvent containing oxygen or halogen atoms. Heptane has a rather low electron density ($\rho_1 z_1 = 0.396$ mol/e cm^{-3}) compared to toluene ($\rho_1 z_1 = 0.470$ mol/e cm^{-3}), but for the actual magnitude of the contrast factor K (see eqs 2 and 3) the partial specific volume ν_2^* of the polymer in the corresponding solvent is of the same importance so that polymer solutions in toluene display an even higher contrast than those in heptane. The values for Δz are collected in Table II. To get an idea of the magnitude of the actual electron densities differences ($\Delta z > 0.14$), comparison with data from previous successful SAXS investigations shows that they are much higher than those of polystyrene in toluene ($\Delta z = 0.109$ mol/e g^{-1}) but are comparable to those of PMMA in acetone ($\Delta z = 0.194$ mol/e g^{-1}).[18,19,67] Consequently, scattering curves for these polymer solutions can be measured by SAXS down to rather low concentrations because of the high contrast.

Figure 9 shows the Zimm diagram of C10PCPS (sample 1), which has been synthesized via the active ester route. The scattering curves showing a pronounced negative curvature in the Zimm plot display the typical angular dependence of the particle scattering factor of rodlike molecules discussed in the previous section. Therefore,

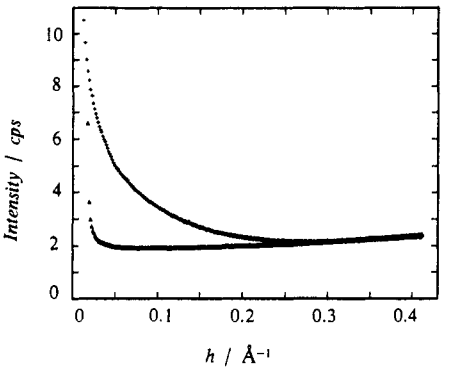

Figure 8. Slit-smeared scattering curves of C10PCPS, sample 1 in heptane at 20 °C: (+) polymer solution, 9.85 mg/mL; (Δ) heptane (7-h measuring time for each scattering curve using an entrance slit width of 80 μm; both curves corrected for absorption).

this is the first experimental hint to a highly extended conformation of these macromolecules. A linear extrapolation of the scattering data for $h = 0$ is not possible and would also be highly erroneous. The more reliable extrapolation method is fitting reciprocal particle scattering functions of rodlike particles to the data, as has been done in the present case. The z-average radius of gyration R_z is obtained from the initial slope of the extrapolated curve. Similar Zimm diagrams showing the same negative curvature of the reciprocal form factor was reported by Coviello et al.[61] for light scattering results from dilute solutions of xanthan, a stiff-chain biopolymer, and by Donkai et al.[68] for measurements on imogolite, a soluble rodlike aluminum silicate.

The extrapolation of the data in Figure 9 gives a weight-average molecular weight of 1.15×10^5 g mol^{-1} and a z-average radius of gyration of 111 Å. The second virial coefficient of the osmotic pressure is zero within the range of experimental error. The nonlinear increase of the apparent molecular weight at higher concentrations is a clear sign to the onset of aggregation phenomena beginning to play a role in this concentration regime. Together with the repeat distance, which is known from X-ray powder diffraction,[37] a weight-average contour length $L_w = 222$ Å is calculated from M_w and the corresponding degree of polycondensation, P_w. If the diameter d of the molecules is considered, which is also taken from X-ray powder diffraction on the bulk samples to avoid the possible influence of a solvate shell, an axial ratio of $L_w/d = 6.3$ is obtained when a rodlike conformation is assumed, which has still to be proven. All relevant data and results from SAXS and density measurements are collected in Table II. The degree of polycondensation of this first sample is still not unexceptionally high although the molecular weight is quite high for a stiff-chain condensation polymer. Technically, relevant condensation polymers have molecular weights typically in the range from 10 000 to 50 000 g mol^{-1}, but when discussing molecular weights of substituted phthalocyaninato–polysiloxanes, it has to be kept in mind that the monomers already have molar masses between 1000 and 3000 g mol^{-1} depending on the side-chain length. Therefore, the relevant quantities for further discussion are the degree of polycondensation, the contour length, and the axial ratio.

As has been discussed in detail previously,[11] the reaction cycle using the active ester route can be repeated to increase the molecular weight of the polymer drastically. Sample 1 from C10PCPS, for which the SAXS results are shown in Figure 9, has been subjected to this treatment. The Zimm diagram of the modified sample (C10PCPS, sample

Table II
Results from SAXS Measurements on Dilute Solutions of Alkoxy-Substituted Phthalocyaninato–Polysiloxanes in Various Solvents at Specified Temperatures

	C10PCPS (I) heptane 20 °C	C10PCPS (II) heptane 20 °C	C1C8PCPS toluene 20 °C	C18PCPS toluene 20 °C	C12PCPS (I) toluene 20 °C	C12PCPS (I) toluene 40 °C	C12PCPS (II)[g] toluene 20 °C
$\nu_2/(cm^3\ g^{-1})$	0.9570	0.9642	0.7468	0.6436	0.8011	0.8211	0.8608
$\Delta z/(mol\ e^{-1})$	0.1673	0.1646	0.1852	0.2530	0.1740	0.1652	0.1460
$M_w/(10^5\ g\ mol^{-1})$	1.18 (0.08)[a]	2.50 (0.20)	0.63 (0.05)	1.89 (0.10)	3.30 (0.25)	3.20 (0.25)	2.00 (0.32)
P_w	65 (5)	139 (11)	53 (5)	69 (4)	162 (12)	157 (10)	98 (16)
$L_w/Å$[b]	222 (15)	472 (36)	176 (6)	239 (12)	555 (42)	539 (39)	337 (54)
$R_z/Å$	111 (9)	240 (20)	98 (7)	102 (7)	241 (22)	229 (28)	184 (31)
$A_2/(10^{-4}\ cm^3\ mol\ g^{-2})$	0	0	2.2 (0.4)	−1.6 (0.3)	−3.8 (0.5)	−3.6 (0.6)	2.0 (0.4)
$M_L(theor)/(g\ mol^{-1}\ Å^{-1})$[c]	538	538	352	782	594	594	594
$M_L(exptl)/(g\ mol^{-1}\ Å^{-1})$	510 (55)	405 (50)	334 (21)	1018 (120)	541 (50)	557 (63)	563 (20)
$R_c/Å$	17 (3)	18 (2)	15 (1)	(≃24)[f]	19 (3)	22 (3)	9 (1)
$r/Å$[d]	24 (4)	25 (3)	21 (2)	(≃34)[f]	27 (4)	31 (4)	13 (2)
L_w/d[e]	6.3 (0.4)	13.4 (1.0)	6.8 (0.2)	5.7 (0.4)	15.4 (1.2)	15.0 (1.1)	9.3 (1.5)

[a] a (b) means $a \pm b$. [b] Calculated from P_w using the repeat distance as determined by X-ray powder diffraction.[37] [c] Calculated from M_w and the repeat distance. [d] Calculated from R_c according to eq 18. [e] Axial ratio where d is the rod diameter as measured by X-ray powder diffraction.[37] [f] No good fit according to eq 15 possible. [g] Sample obtained from Dr. van der Pol, University of Utrecht, The Netherlands.

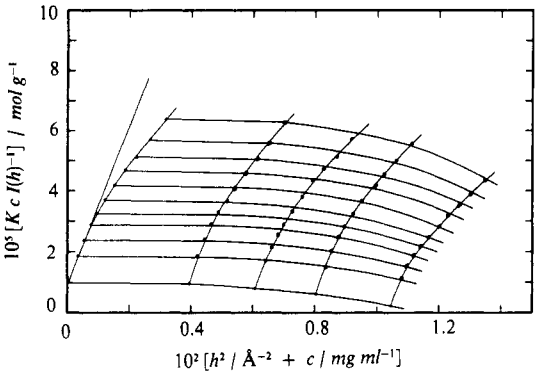

Figure 9. Zimm diagram of C10PCPS (sample 1) in heptane at 20 °C.

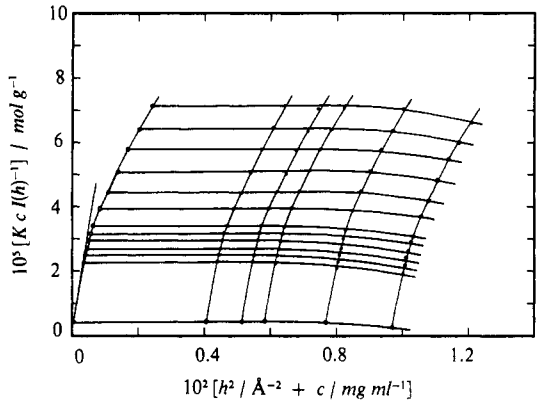

Figure 10. Zimm diagram of C10PCPS (sample 2) in heptane at 20 °C.

2) is shown in Figure 10. The molecular weight has nearly doubled ($M_w = 2.5 \times 10^5$ g mol^{-1}). This result demonstrates that this particular polycondensation method is suitable to produce really high molecular weight, soluble phthalocyaninato–polysiloxanes, which were not available before, but Figure 10 also demonstrates the inherent problems of the SAXS method when investigating high M_w polymers. Since the lower limit for the scattering vector h of the Kratky camera is limited by the way in which residual primary beam intensity can be eliminated from the scattering curves (compare Figure 8), the Zimm extrapolation can be subject to large errors if not enough data points can be measured in the low h range. By further optimization of the camera adjustment, measurements could be extended down to $h = 0.006$ Å^{-1} (corresponding to a Bragg value of about 1000 Å) using an entrance slit

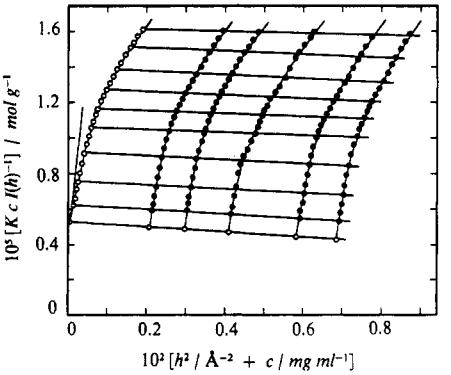

Figure 11. Zimm diagram of C18PCPS in toluene at 20 °C.

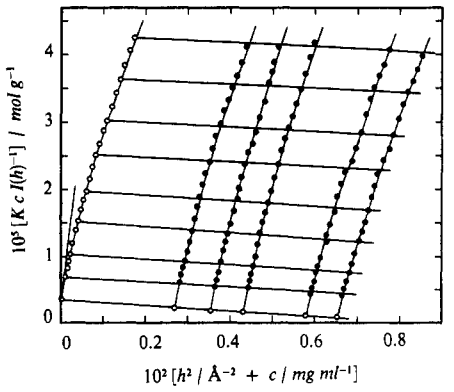

Figure 12. Zimm diagram of C12PCPS in toluene at 20 °C.

of 80 μm for the whole scattering curve. Systematic errors by combining different parts of the scattering curve measured with different entrance slit widths could therefore be prevented.

Figures 11 and 12 show the Zimm diagrams of C18PCPS and C12PCPS measured in toluene at 20 °C. Both polymers were synthesized by using halogenophilic trifluoromethanesulfonates as condensation reagents. The molecular weights of these two samples are 1.89×10^5 and 3.33×10^5 g mol^{-1}, respectively. These values are in the same range as those for samples prepared by the active ester method. Again Table II summarizes all results for these polymers. The measurement of C12PCPS in toluene at elevated temperature (40 °C) did not result in any particular difference in the scattering curves and the derived molecular parameters (see Table II).

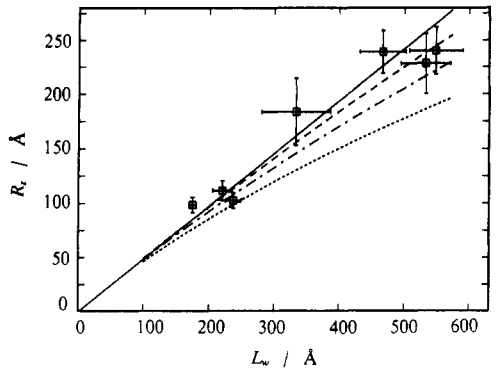

Figure 13. Plot of the experimental radii of gyration R_z as a function of the contour length L_w and theoretical curves for (a) rigid rods with $U = 0.83$ (—); (b) wormlike chains with $U = 1$ and a persistence length of 1000 Å (- - -), 500 Å (– · –) and 250 Å (···) according to eq 21.

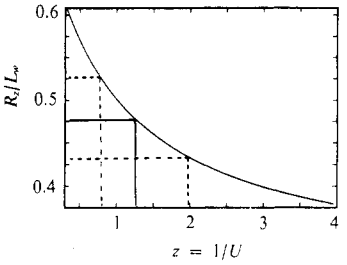

Figure 14. Ratio of the radius of gyration over contour length as a function of the reciprocal polydispersity z. The experimental result for rigid rods from Figure 13 is marked together with its error band.

The plot of the z-average radius of gyration as a function of the contour length L_w is shown in Figure 13. This type of plot is usually used in the interpretation of light scattering data to evaluate the chain stiffness in terms of the persistence length because of the limited scattering vector range of this method. The data can be fitted with a straight line using eq 22. Linear regression analysis gives a slope of 0.48 ± 0.05. If the ratio R_z/L_w is plotted as a function of the reciprocal polydispersity $z = 1/U$ according to eq 22 (Figure 14), the linear slope from the previous plot can be used to determine the mean polydispersity of the substituted phthalocyaninato-polysiloxanes directly from this graph. For the present data we obtain $U = M_w/M_n - 1 = 0.83 \pm 0.40$. The error is quite large since evaluation takes place in a region where the function $R_z/L_w = f(1/U)$ displays a rather steep slope. But, nevertheless, this result is quite reasonable for a condensation polymer. Close inspection of the data in Figure 13 also leads to a further interesting feature: the experimental data can also be approximated in the range of their experimental errors using eq 21 for semiflexible, wormlike chains when the persistence length as fit parameter is chosen large enough. As exemplified in Figure 13, the results obtained in this work do not allow us to distinguish unambiguously between a rodlike and a wormlike conformation with a persistence length equal to or larger than 1000 Å when using the relation $R_z = f(L_w)$. The reason for this deficiency follows from the investigations of Schmidt.[57] If a chain stiffness is assumed with a lower limit of 1000 Å for the presistence length (corresponding to a Kuhn length of 2000 Å), all polymer samples measured have a weight-average contour length much smaller than one Kuhn length (see L_w data in Table II). The influence of increasing flexibility on the radius of gyration leads only to minor deviations from the values of the corresponding rods in the range of contour lengths considered here. The experimental errors of L_w and R_z, which are typically about

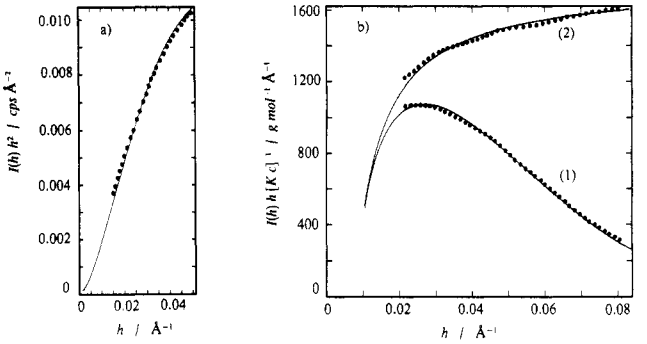

Figure 15. Comparison of experimental SAXS data of C10PCPS, sample 1, in heptane (points) with particle scattering functions of cylindrical particles (solid lines): (a) Kratky plot, (b) Holtzer plot of the desmeared SAXS data (1) and after correction for finite thickness (2). Particle scattering functions were calculated by using eq 17 with $U = 1$.

10%, smear our this tiny effect. Therefore, a distinction between the two conformational models is not possible in this region because of principal reasons. Only a lower estimate of the persistence length of $q \geq 1000$ Å can be given for sure. A more precise determination of q using the $R_z - L_w$ relation can only be obtained if a large molecular weight range is covered. This is definitely not the case in the present investigation. Furthermore, this method for data interpretation, although frequently used, is a rather indirect technique to determine the chain stiffness and is therefore subject to large errors when L_w and R_z cannot be determined to a high degree of accuracy.

Far more direct information about chain conformation in dilute solution can be obtained by fitting theoretical form factors to the experimental data over a wide angular range, which cannot be obtained by light scattering. Figure 15 shows the Kratky and Holtzer plots of C10PCPS with $M_w = 1.18 \times 10^5$ g mol$^-$ (sample 1). The Kratky plot (Figure 15a) shows a linear behavior for $h < 0.04$ Å^{-1}, which is typical for rodlike particles. The corresponding theoretical form factor was calculated according to eqs 16 and 17 using $U = M_w/M_n - 1 = 1$ and all other parameters as given in Table II for this particular sample. The slope of the linear part of this curve is proportional to the mass per unit contour length, M_L. A deviation of the data from the theoretical curve at low scattering angles in the sense of a Gaussian scattering component, which is clearly not present here, would be a sign for a finite persistence length. The deviation from the linear behavior at $h \geq 0.04$ Å^{-1} is a clear hint to the finite thickness of the rodlike macromolecules. The cross-sectional dimension is obtained from the Holtzer plot in Figure 15b where the data have been plotted according to eq 24. The experimental data together with the theoretical form factor using again the parameters in Table II are given in curve 1. A logarithmic plot of the ratio $I(h)h/Kc$ versus h^2 gives the radius of gyration of the cross-section, which is $R_c = 17 \pm 3$ Å for the example discussed here. The cross-section factor according to eq 15 can be eliminated, subsequently resulting in the particle scattering function of the corresponding infinitely thin rod in the Holtzer presentation. The experimental data modified in this way (curve 2) can be easily approximated by using eq 13. The fit parameters are the mass per unit length, M_L, and the number-average contour length, L_n. Within the experimental error the resulting value $M_L = 510 \pm 55$ g mol^{-1} Å^{-1} agrees well with the theoretical value M_L(theor) = 538 g mol^{-1} Å^{-1}, which has been calculated from the molar mass of the repeat unit and the repeat distance along the polymer chain. The ratio L_w/L_n was found to be about 2, which is in agreement with previous

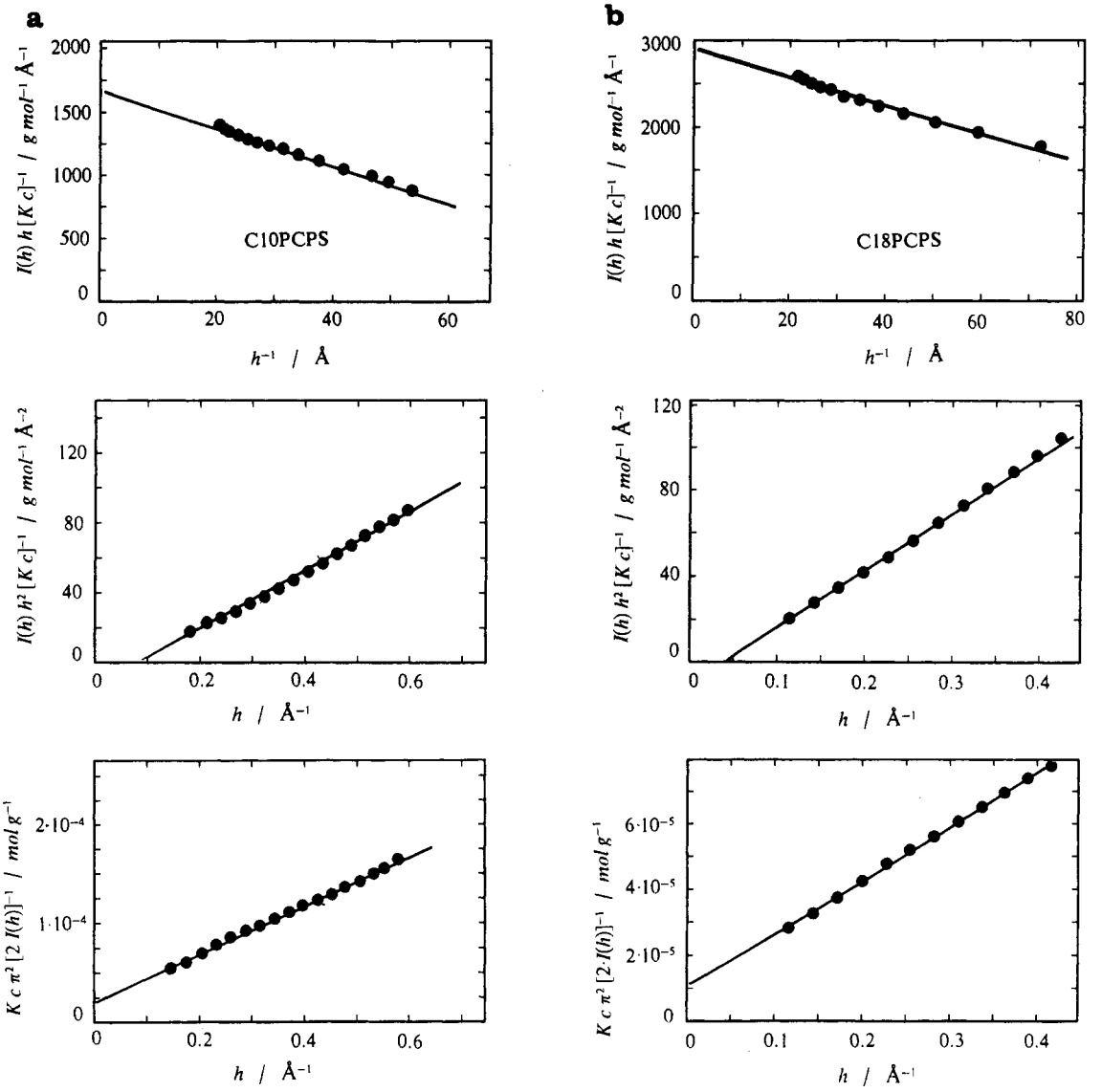

Figure 16. Linear plots of the desmeared SAXS data of C10PCPS, sample 1, in heptane (a) and C18PCPS in toluene (b) according to the functions defined in Table I.

estimates of the polydispersity. The SAXS data from all other samples were evaluated in the same way, and the results are compiled in Table II.

Methods for obtaining linear plots are summarized in Table I. In Figure 16 the experimental data of two different polymer samples are plotted according to these relations after the finite cross-section has been eliminated as discussed above. The intensity data were taken from the corresponding Zimm diagrams for infinite dissolution to avoid concentration effects. As can be seen by comparison of Figures 6 and 16, the data used for the linear plots are restricted to an angular region where the cross-section of the macromolecules still does not have a very large influence. So the results will not be affected much by a wrong R_c value. All plots in Figure 16 show rather nice linear fits, and the values of M_L, M_n, and L_n calculated from slope and intercept (compare Table I) are collected in Table III. All values are in the range expected from the conventional Zimm analysis, although obvious deviations of the approximate form factor from the angular dependence of the exact one have been identified in this angular region (see Figure 6). M_L values show good agreement with those obtained by the Holtzer plot according to eq 24, which is not surprising since their evaluation is based on the same particle scattering function. As mentioned earlier, the number-average quantities M_n and L_n allow for the determination of the polydispersity when combined with the corresponding weight-average data according to Table II. For the examples discussed here we find U = 1.31 (C10PCPS, sample 1) and 0.87 (C18PCPS). These values are well within the range of the results obtained by application of eq 22.

As can be seen from Figure 16 and the previous discussion, the application of the linear relations given in Table I is limited at large scattering angles even if R_c is known exactly since the Guinier-type approximation for the cross-section (eq 15) is only valid within a limited h range. Also the intramolecular, liquidlike scattering of the macromolecules increases at high h values where it can overlay the pure particle scattering.

Discussion

Inspection of the molecular weights of the polymer samples investigated here demonstrates that the polycondensation can be run to rather high conversion even in spite of the additional steric constraint imposed by the alkoxy side chains when using appropriate reactions conditions. The degrees of polymerization obtained are in the range of those reported for the parent, unsubstituted polymer[69,70] prepared by high-temperature poly-

Table III
Results from Linear Plots of the Scattering Data from Substituted Phthalocyanonato–Polysiloxanes Corrected for Finite Cross-Section

sample	R_c, Å	method[a]	M_n, 10^5 g mol^{-1}	L_n, Å	M_L, g mol^{-1} Å^{-1}
C18PCPS	24	a	(0.97)[b]	123	955
(toluene 20 °C)		b	0.91	(115)[c]	982
		c	0.91	(115)[c]	982
mean values			1.01	125	959
C10PCPS(I)	17	a	(0.57)[b]	108	541
(toluene 20 °C)		b	(0.38)[b]	72	503
		c	0.56	(105)[c]	542
mean values			0.51	95	529

[a] See Table I. [b] Calculated from L_n. [c] Calculated from M_n.

condensation in the bulk. Compared to earlier attempts to synthesize substituted phthalocyaninato–polysiloxanes,[4-8] the results obtained in this investigation show that the improved synthetic procedures reported recently[10,11] are well suited to produce also high molecular weight derivatives of this polymer soluble in common organic solvents. Furthermore, qualitative statements concerning the degree of polymerization derived from UV/vis spectra of these polymers[11,13] find their quantitative confirmation in the results from this investigation.

The evaluation of the angular dependence of the measured scattering curves shows such a good agreement with theoretical particle scattering functions for polydisperse rods of finite thickness that we suggest this as an experimental proof of the rodlike nature of these compounds. Although there is no fixed limit between rodlike and semiflexible chains in terms of a single number for the persistence length, and many different classifications are given throughout literature, we give such a definition to clarify this discussion. From a practical point of view a molecule should be defined rodlike rather than semiflexible when the chain conformation can be described with the form factor of a rigid rod within the experimental range of error. Assuming that the ratio q/L_w can be determined to an accuracy of 5–10% by conventional techniques, the two conformational models become indistinguishable when $q/L_w \gtrsim 4$.[57] This value may be considered as tentatively defining the limit between rodlike and semiflexible chains. So compared to other conformational studies on polymers, our results are quite remarkable since there have been no experimental proofs for rodlike conformations of soluble synthetic polymers so far, especially in the field of stiff-chain liquid-crystalline and also conjugated polymers. Experimental data on the chain stiffness of these materials suggest that they are not rodlike at all in the strict sense of the above definition but typically show persistence lengths in the range from 100 to 1000 Å.[71,72] Moreover, from the work of Krigbaum and Ciferri et al.,[73-75] it follows that extreme chain stiffness is not required to obtain liquid-crystalline phases over a wide temperature range. The more important molecular feature in this regard is the axial ratio of the Kuhn segment rather than that of the contour length, but since most theories of the liquid-crystalline state assume a rodlike symmetry of the particles involved, the polymers investigated here present appropriate materials to test these theories without facing the problem of additional internal flexibility. Furthermore, the anisotropy in terms of the axial ratio can be varied over a wide range depending on the side-chain length and the molecular weight, which define the diameter and the contour length of the macromolecule.

The axial ratio L_w/d given in Table II, which is as well a weight average as the corresponding contour length L_w, is a quantitative measure of this anisotropy. A generally accepted lower limit of this value, which has to be exceeded to achieve liquid crystallinity, cannot be given. Most authors refer to the value of 6.42 given by Flory,[76,77] which has been derived for athermic mixtures of rodlike molecules with a low molecular weight solvent, but many materials show liquid-crystalline phases if an axial ratio of the rigid chain segment of about 3–4[73,74] is reached. Exactly the same situation is found in the present case where all derivatives with $n \geq 10$ show transitions to liquid-crystalline phases, the properties of which will be discussed elsewhere.[37] Even in the case of C18PCPS, where the number-average axial ratio is only about 3 when a polydispersity of $U = 1$ is assumed, a mesophase stable up to very high temperatures (about 200 °C) is observed.

The mass per unit length, M_L, is a very important result from the interpretation of the experimental scattering curves since it gives information about possible aggregation phenomena. Aggregation of stiff-chain polymers in solution is a major problem in their analytical characterization and the possible cause of much misinterpretation of their dilute-solution properties. The M_L values found in this work are in the range of the corresponding theoretical values or even a little bit lower, which is expected because of the asymptotic nature of the underlying theoretical relations. Only in the case of C18PCPS is the experimental M_L value significantly higher than the theoretical one. From these findings aggregation in the form of parallel aligned rodlike molecules can be ruled out (except for C18PCPS). End-to-end aggregates that might be present through specific end-group interactions are not monitored by M_L, but there is no obvious reason to assume such interactions or the stability of such aggregates. Consequently, we believe that the results obtained from our investigations really represent properties of the isolated macromolecule.

From the evaluation of the cross-sectional dimension, the question arises as to how the radius r of the homogeneous cylinder derived from the radius of gyration of the cross-section R_c is related to the real radius of the actual molecule as determined by X-ray powder diffraction from the bulk polymers. Comparison of the data shows that radii derived from SAXS are about 50% larger than the corresponding bulk values. This finding seems reasonable since the solvent shell around the molecule has generally an electron density different from that of the pure solvent. It therefore contributes to the excess scattering. The magnitude of this effect generally cannot be determined from SAXS measurements in only a single solvent. Contrast variation, e.g., measurement of the same polymer in different solvents having different electron densities, is required to determine a particle scattering function independent from solvation effects.[15,78,79] Such a form factor then also reproduces the pure intramolecular liquidlike scattering of the polymer molecule at high h values, which would allow us to analyze for the local distribution of scattering centers rather than approximate the molecule by a homogeneous cylinder. Such contrast variation measurements using conventional SAXS equipment are very delicate, and therefore most work in this field has been done by using SANS[15] since this method offers much easier possibilities to vary the scattering contrast. Furthermore, no such investigations have been reported for synthetic polymers so far. For the angular region investigated in this work the continuous chain limit represents a fairly good approximation.

Comparison of the results for C12PCPS (sample 1) measured at 20 and 40 °C in toluene does not show any

significant temperature effect (Table II). Indeed, no changes in the scattering curve are expected since there is no aggregation at room temperature that might be surpressed when raising the temperature. So molecular weights and radii of gyration are essentially the same at both temperatures. Furthermore, the form of the scattering curves remains the same, which leads to the conclusion that within the resolution of the method no thermally induced increase in flexibility of the main chain takes place. The rodlike nature of the main chain remains unaltered, whereas in semiflexible polymers the persistence length shows a pronounced negative temperature coefficient that is typically of the order of magnitude of $d(\ln q)/dT = 0.005–0.01\ K^{-1}$.[73,74] In the same way the solvent quality in terms of the second virial coefficient of the osmotic pressure, A_2, does not change in this moderate temperature range. Interesting to note are the differences to the second samples of C12PCPS, which has been synthesized by a modified bulk polycondensation procedure.[80] The radius of gyration of the cross-section for this sample is significantly smaller, and, in contrast to the results for sample 1, a positive value for A_2 is found. The same finding is observed for the unsymmetrically substituted C1C8PCPS. This leads to the conclusion that during the bulk polycondensation, which takes place above 200 °C,[80] a partial loss of side chains might occur, which could take account of these discrepancies. Thermogravimetric measurements[37] give further evidence for such processes in this temperature range. For a final explanation of these differences, further analytical data for this particular sample are needed.

At different stages of this investigation we have given estimates on the polydispersity of the polymers as derived from the scattering curves. As mentioned above, these values are well within the range of the most probable distribution ($U = 1$) expected for condensation polymers, but this does not imply that these are exact values. As discussed in the theoretical section of this paper, one has to keep in mind how these results have been obtained. The underlying model is the scattering from rodlike particles. As outlined above, a small, finite flexibility that is equivalent to a high persistence length (in contrast to an infinite persistence length for a rod) has a drastic effect on the results for the polydispersity, since we cannot distinguish unambiguously between the rod and the slightly flexible chain in the molecular weight range studied here, but from the angular dependence of the scattering curves, the rigid-rod model is clearly favored. Futhermore, the type of distribution function used for the analysis also influences the results. Its monomodal nature has been verified by preliminary GPC studies but not the exact form of the distribution function. A complete particle size distribution function could be obtained from the scattering curve if the exact form factor of the monodisperse particle is known.[81]

A final comment on the linear data interpretation methods has to be made. Linear fits are clearly preferred since they can be done without much computational effort, but, as mentioned earlier, the linear relations given in Table I are asymptotic in nature, and they can only be applied when the cross-sectional dimension has been eliminated. It follows that a conventional Zimm analysis according to eq 1, although not linear, is by no means less accurate than the linear methods for the determination of the molecular weight and other molecular parameters. We think that the very best results can be obtained if all these methods are applied simultaneously and the consistency of the results is checked. This procedure, as demonstrated above, it also the best way to analyze for the chain conformation in the rigid-rod limit.

Concluding Remarks

This investigation shows that SAXS measurements from dilute polymer solutions can give the complete information on the molecular dimensions of a polymer that cannot be investigated by light scattering because of strong absorption over the entire visible spectrum. Additional information, e.g., the local chain conformation, can be deduced directly from the scattering curves since a wide range of the scattering vector is covered by this method. On the other hand, this technique is clearly limited concerning really high molecular weight materials. Also the necessity to desmear the scattering data obtained by a slit collimation camera is a clear disadvantage of the technique.

The variety of molecular parameters that have a distinct influence on the scattering behavior renders an unambiguous data analysis rather complex. The interdependence of the influences is also the cause for quite large experimental errors in the derived quantities. Still, the possibility to obtain the same piece of information from different parts of the same spectrum of scattered radiation offers the opportunity to check for the consistency of the results and therefore for the applicability of plausible chain models.

Acknowledgment. We gratefully thank J. F. van der Pol and Prof. W. Drenth, University of Utrecht, The Netherlands, for providing a polymer sample, Dr. M. Schmidt, Dr. M. Ballauff, and Prof. E. W. Fischer for many helpful discussions and M. Steiert and Dr. V. Enkelmann for technical assistance. This work was supported by the Bundesminister für Forschung und Technologie under the project "Steife Makromoleküle".

References and Notes

(1) Marks, T. J. *Science* **1985**, *227*, 881.
(2) Ciliberto, E.; Doris, K. A.; Pietro, W. J.; Reisner, G. M.; Ellis, D. E.; Fragala, I.; Herbstein, F. H.; Ratner, M. A.; Marks, T. J. *J. Am. Chem. Soc.* **1984**, *106*, 7748.
(3) Swift, D. R. Ph.D. Thesis, Case Western University, Cleveland, OH, 1970.
(4) Metz, J.; Pawlowski, G.; Hanack, M. *Z. Naturforsch.* **1983**, *38B*, 378.
(5) Sirlin, C.; Bosio, L.; Simon, J. *J. Chem. Soc., Chem. Commun.* **1988**, 236.
(6) Sirlin, C.; Bosio, L.; Simon, J. *Mol. Cryst. Liq. Cryst.* **1988**, *155*, 231.
(7) Orthmann, E.; Wegner, G. *Makromol. Chem. Rapid Commun.* **1986**, *7*, 243.
(8) Orthmann, E. Ph.D. Thesis, University of Mainz, Mainz, FRG, 1986.
(9) Sauer, T.; Wegner, G. *Makromol. Chem. Macromol. Symp.* **1989**, *24*, 303.
(10) Caseri, W.; Sauer, T.; Wegner, G. *Makromol. Chem., Rapid Commun.* **1988**, *9*, 651.
(11) Sauer, T.; Caseri, W.; Wegner, G., submitted for publication in *Macromolecules*.
(12) Burchard, W. *Adv. Polym. Sci.* **1983**, *48*, 1.
(13) Sauer, T.; Caseri, W.; Wegner, G. *Mol. Cryst. Liq. Cryst.* **1990**, *183*, 387.
(14) Glatter, O.; Kratky, O. *Small-Angle X-Ray Scattering*; Academic Press: New York, London, 1982.
(15) Feigin, A.; Svergun, D. I. *Structure Analysis by Small-Angle X-Ray and Neutron Scattering*; Plenum Press: New York, 1987.
(16) Kratky, O. *Prog. Biophys.* **1963**, *13*, 105.
(17) Pilz, I. In *Principles and Techniques in Protein Chemistry*; Leach, S. J., Ed.; Academic Press: New York, London, 1973.
(18) Kirste, R. G.; Wunderlich, W. *Makromol. Chem.* **1964**, *73*, 240.
(19) Wunderlich, W.; Kirste, R. G. *Ber. Bunsen-Ges. Phys. Chem.* **1964**, *68*, 646.
(20) Kirste, R.; Oberthür, R. C. In *Small-Angle X-Ray Scattering*; Glatter, O., Kratky, O., Eds.; Academic Press: New York, London, 1982.

(21) Higgins, J. S.; Stein, R. S. *J. Appl. Cryst.* **1978**, *11*, 346.
(22) Richards, R. W. *J. Macromol. Sci., Chem.* **1989**, *A26*, 787.
(23) Ragnetti, M.; Oberthür, R. C. *Colloid Polym. Sci.* **1986**, *264*, 32.
(24) Aime, J. P.; Rawiso, M.; Schott, M. In *Electronic Properties of Conjugated Polymers*; Kuzmany, H., Mehring, M., Roth, S., Eds.; Springer: Berlin, 1987.
(25) Rawiso, M.; Aime, J. P.; Fave, J. L.; Schott, M.; Müller, M. A.; Schmidt, M.; Baumgartl, H.; Wegner, G. *J. Phys. Fr.* **1988**, *49*, 861.
(26) Stabinger, H.; Kratcky, O. *Makromol. Chem.* **1978**, *179*, 1655.
(27) Glatter, O. *J. Appl. Cryst.* **1977**, *10*, 415.
(28) Glatter, O. *Acta Phys. Aust.* **1977**, *47*, 83.
(29) Zimm, B. H. *J. Chem. Phys.* **1948**, *16*, 1093.
(30) Oberthür, R. C. Ph.D. Thesis, University of Mainz, Mainz, FRG, 1974.
(31) Garg, S. K.; Stivala, G. S. *J. Polym. Sci., Polym. Phys. Ed.* **1978**, *16*, 1419.
(32) Neugebauer, T. *Ann. Phys.* **1943**, *42*, 34.
(33) Zimm, B. H.; Stein, R. S.; Doty, P. *Polym. Bull.* **1945**, *1*, 90.
(34) Porod, G. *Acta Phys. Aust.* **1948**, *2*, 255.
(35) Zimm, B. H. *J. Chem. Phys.* **1948**, *16*, 1099.
(36) Holtzer, A. *J. Polym. Sci.* **1955**, *17*, 432.
(37) Sauer, T.; Wegner, G., to be submitted for publication.
(38) Kratky, O. *Z. Elektrochem.* **1956**, *60*, 245.
(39) Luzzati, V. *Acta Crystallogr.* **1960**, *13*, 939.
(40) Kirste, R. *Z. Phys. Chem.* **1963**, *36*, 265.
(41) Hayashi, H.; Flory, P. J. *Macromolecules* **1987**, *16*, 1328.
(42) Rawiso, M.; Duplessix, R.; Picot, C. *Macromolecules* **1987**, *20*, 630.
(43) Koyama, R. *J. Phys. Soc. Jpn.* **1974**, *36*, 1409.
(44) Guinier, A.; Fournet, G. *Small-Angle Scattering of X-Rays*; Wiley: New York, 1955.
(45) Holtzer, A.; Rice, S. A. *J. Am. Chem. Soc.* **1957**, *79*, 4847.
(46) Hjelm, R. P. *J. Appl. Crystallogr.* **1985**, *18*, 452.
(47) Mittelbach, P.; Porod, G. *Acta Phys. Aust.* **1961**, *14*, 405.
(48) Porod, G. *Monatsh. Chem.* **1949**, *80*, 251.
(49) Kratky, O.; Porod, G. *Recl. Trav. Chim. Pays-Bas* **1949**, *68*, 1106.
(50) Flory, P. J. *Statistical Mechanics of Chain Molecules*; Interscience Publishing: New York, 1969.
(51) Burchard, W.; Kajiwara, K. *Proc. R. Soc. London* **1970**, *A36*, 185.
(52) Norisuye, T.; Murakama, H.; Fujita, H. *Macromolecules* **1978**, *11*, 966.
(53) Hays, J. B.; Magar, M. E.; Zimm, B. H. *Biopolymers* **1969**, *8*, 531.
(54) Schmid, C. W.; Rinehart, F. P.; Hearst, J. E. *Biopolymers* **1971**, *10*, 883.
(55) Arpin, M.; Strazielle, C. *Polymer* **1977**, *18*, 591.
(56) Wenz, G.; Müller, M. A.; Schmidt, M.; Wegner, G. *Macromolecules* **1984**, *17*, 837.
(57) Schmidt, M. *Macromolecules* **1984**, *17*, 553.
(58) Zero, K.; Aharoni, S. M. *Macromolecules* **1987**, *20*, 1957.
(59) Schmidt, M.; Paradossi, G.; Burchard, W. *Makromol. Chem., Rapid Commun.* **1985**, *6*, 767.
(60) Koyama, R. *J. Phys. Soc. Jpn.* **1973**, *34*, 1029.
(61) Coviello, T.; Kajiwara, K.; Burchard, W.; Dentini, M.; Creszenzi, V. *Macromolecules* **1986**, *19*, 2826.
(62) Benoit, H.; Doty, P. *J. Phys. Chem.* **1953**, *57*, 958.
(63) Oberthür, R. C. *Makromol. Chem.* **1978**, *179*, 2693.
(64) Kirste, R. *Z. Phys. Chem.* **1964**, *42*, 351.
(65) Berry, G. C. *J. Chem. Phys.* **1966**, *44*, 4550.
(66) Goldstein, M. *J. Chem. Phys.* **1953**, *21*, 1255.
(67) Wild, G. Ph.D. Thesis, University of Mainz, Mainz, FRG, 1967.
(68) Donkai, N.; Inagaki, H.; Kajiwara, K.; Urakawa, H.; Schmidt, M. *Makromol. Chem.* **1985**, *186*, 2623.
(69) Dirk, C. W.; Inabe, T.; Schoch, K. F.; Marks, T. J. *J. Am. Chem. Soc.* **1983**, *105*, 1539.
(70) Diel, B. N.; Inabe, T.; Lyding, J. W.; Schoch, K. F.; Kannewurf, C. R.; Marks, T. J. *J. Am. Chem. Soc.* **1983**, *105*, 1551.
(71) Tsvetkov, V. N.; Shtennikova, I. N. In *Polymeric Liquid Crystals*; Blumstein, A., Ed.; Plenum Press; New York, 1985.
(72) Kwolek, S. C.; Morgan, P. W.; Schaefgen, J. R. In *Encyclopedia of Polymer Science and Engineering*; Mark, H., Bikales, N. M., Overberger, C. G., Menges, G., Eds.; Wiley & Sons: New York, 1985; Vol. 9, p 1.
(73) Krigbaum, W. R.; Brelsford, G.; Ciferri, A. *Macromolecules* **1989**, *22*, 2487.
(74) Ciferri, A.; Marsano, E. *Gazz. Chim. Ital.* **1987**, *117*, 567.
(75) Conio, G.; Bianchi, E.; Ciferri, A.; Krigbaum, W. R. *Macromolecules* **1984**, *17*, 856.
(76) Flory, P. J. *Proc. R. Soc. London* **1956**, *A234*, 73.
(77) Flory, P. J. *Adv. Polym. Sci.* **1984**, *59*, 1.
(78) Stuhrmann, H. *Z. Phys. Chem.* **1970**, *72*, 177.
(79) Stuhrmann, H. *Z. Phys. Chem.* **1970**, *72*, 185.
(80) van der Pol, J. F., private communication.
(81) Glatter, O. *J. Appl. Crystallogr.* **1980**, *13*, 7, 577.